Finding streams using action-angle coordinates

Paul McMillan & James Binney

We describe a new method for finding substructure (e.g. accreted satellite galaxies) in surveys of the Solar neighbourhood. It relies upon finding the action-angle coordinates for stars, which we achieve using the "torus method" (e.g. McGill & Binney 1990). We analyse pseudo-data from a simulation of a disrupted satellite galaxy in the potential of the Milky Way, and find that stars near the Sun are confined to patches in action (or frequency) space. We also introduce a diagnostic allowing us to use satellite remnants to rule out incorrect Galactic potentials, and determine when the satellite was disrupted.

Action-Angle coordinates

For a regular orbit the three actions J_i are conserved, and the conjugate action coordinates θ_i increase linearly with time:

$$\theta_i(t) = \theta_i(0) + \Omega_i(\mathbf{J})t$$

with Ω_i the frequencies (which depend only on **J**). The conventional phase-space coordinates (x,v) are 2π-periodic in the angles. Hence in J-θ space, a bound orbit moves only in θ, on a surface which is topologically a torus. The actions are also adiabatic invariants.

The torus method involves distorting the tori corresponding to orbits in the isochrone potential (for which θ and J are known analytically), until they correspond to orbits in the potential of interest.

We restrict ourselves to orbits in axisymmetric potentials, when $J_\phi = L_z$, the z-component of angular momentum.

The simulation data

We follow the disruption and phase-mixing of a self-gravitating satellite in a Galactic potential taken from Dehnen & Binney 1998. The satellite is placed at apocentre (R ~ 9.3kpc) in an orbit in the plane of the galaxy that has pericentre at R ~ 3.1kpc. After 4.5Gyr the remnants from the satellite are well phase-mixed (see Figure 1).

We focus on stars found within 1.5kpc of what we consider the Sun's position, at R=8kpc (red ring in Figure 1). This reflects the situation in real surveys, which are limited to nearby stars.

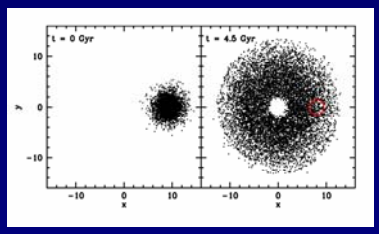

Figure 1: Particle positions in the plane of the Galaxy. We analyse particles within 1.5kpc of the Sun after 4.5Gyr of evolution (indicated by the red ring, right panel)

Analysis in action-angle coordinates

We plot the distribution in **Ω**- and **J**-space of particles within 1.5kpc of the sun after 4.5Gyr (Figure 2). **Ω** and **J** were found in the *same* Galactic potential as was used for the N-body simulation.

In Figure 2 we plot $\Omega t/2\pi$, the number of periods (radial or azimuthal) that our orbit model implies to have occurred since the start of the simulation. Patches of particles are found at near-integer intervals in $\Omega_\phi t/2\pi$, and more frequent intervals in $\Omega_R t/2\pi$. This is because they are all near one point both at the present time and initially. (There is no such effect in Ω_z, because the satellite orbit was in the plane)

This split into patches is also seen in J (Figure 2, right), because Ω is a function of J. The separation of these patches is clearer in other projections of **J**-space, as the individual components of Ω are functions of all 3 components of J.

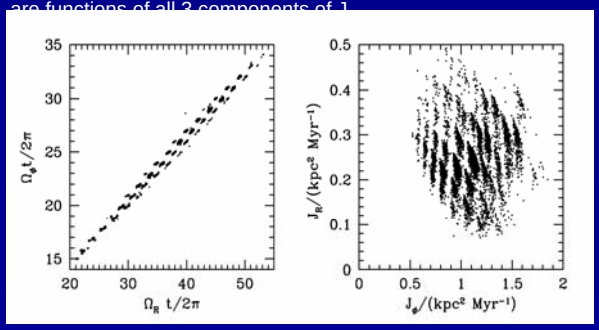

Figure 2: Number of azimuthal periods plotted against number of radial periods (left), and J_R plotted against J_ϕ (right), as determined in the true potential. The values of Ω and J are divided into patches because of the limited volume of real space that is sampled.

The velocity and distance information required to do this analysis for local stars is currently available for the Geneva-Copenhagen sample and (using photometric distances) from RAVE. Gaia data will make it possible for a far larger number of stars. However, the true potential that the stars moved in is (and will not be) exactly known. We need to ensure that this will not disguise the structure seen in Figure 2.

We also determine the frequencies and actions of the particles assuming an incorrect potential (a Miyamoto-Nagai potential, see Figure 3). While the frequencies and actions are now incorrect (the frequencies to a greater extent than the actions), the same split into patches is observed. This ensures that it is possible to identify a satellite, even if we do not know the exact potential.

Further, we can use this technique to rule out the incorrect potential, by exploiting the linear increase of the angles with time, and their 2π-periodicity. We assume that all the particles started with approximately the same values for the angles, and therefore by minimising the average of the statistic δ (see box) for particles from the satellite with respect to t and θ_0, we can determine when and where the satellite was disrupted. For these data, $\theta_{(t=0)}$ is known, so we only need to vary t. In the incorrect potential we see no strong minima, whereas with the true potential we see strong minima at the correct age (Figure 4).

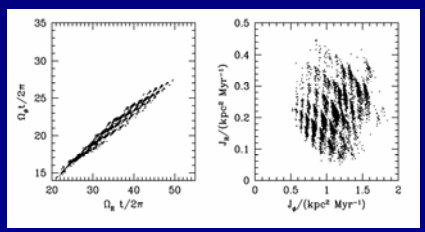

Figure 3: As Figure 2, except with Ω and J determined in an incorrect potential (a Miyamoto-Nagai potential with a similar circular speed at R_0 as the true potential). The split into various patches is still observed, which is reassuring, as it ensures this will be a helpful technique for real data, when the true potential is unknown.

$$\delta_i = \left| \frac{1}{\pi}[\Omega_i t - (\theta_i - \theta_{i,(t=0)}) - 2\pi m_i] \right|$$

With m_i an integer, chosen to minimise δ_i

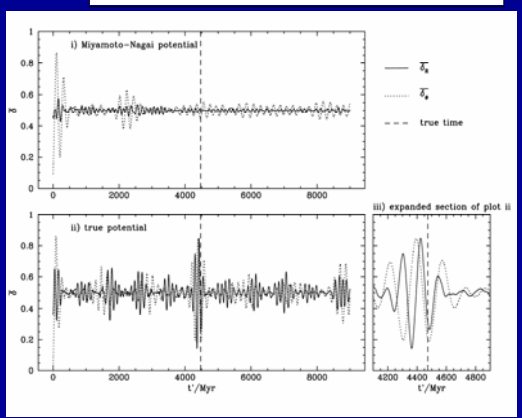

Figure 4: Average of δ_R and δ_ϕ (see box above) over all particles as a function of t. For the true potential, there are strong minima at the true age. For the wrong potential there are none.

For more details see McMillan & Binney 2008 (arxiv:0806.0319)